Research Article | Vol. 31, No. 8 / 10 Apr 2023 / Optics Express 12463

Optics EXPRESS

Diode-pumped mode-locked Yb:Sc_2SiO_5 laser generating 38 fs pulses

LULU DONG,[1] ZHANG-LANG LIN,[2] PAVEL LOIKO,[3] YICHEN LIU,[1] GE ZHANG,[2] HUANG-JUN ZENG,[2] WEN-ZE XUE,[2] SHANDE LIU,[4] LIHE ZHENG,[5] LIANGBI SU,[6] XAVIER MATEOS,[7] HAIFENG LIN,[8] VALENTIN PETROV,[9] LI WANG,[9] AND WEIDONG CHEN[2,9,*]

[1]School of Science, Qingdao University of Technology, 266525 Qingdao, China
[2]Fujian Institute of Research on the Structure of Matter, Chinese Academy of Sciences, 350002 Fuzhou, China
[3]Centre de Recherche sur les Ions, les Matériaux et la Photonique (CIMAP), UMR 6252 CEA-CNRS-ENSICAEN, Université de Caen, 6 Boulevard Maréchal Juin, 14050 Caen Cedex 4, France
[4]College of Electronic and Information Engineering, Shandong University of Science and Technology, 266590 Qingdao, China
[5]School of Physics and Astronomy, Yunnan University, 650091 Kunming, China
[6]State Key Laboratory of High Performance Ceramics and Superfine Microstructure, Shanghai Institute of Ceramics, Chinese Academy of Sciences, 201899 Shanghai, China
[7]Universitat Rovira i Virgili, URV, Física i Cristal·lografia de Materials, (FiCMA)- Marcel·lí Domingo 1, 43007 Tarragona, Spain
[8]College of Physics and Optoelectronic Engineering, Shenzhen University, 518118 Shenzhen, China
[9]Max Born Institute for Nonlinear Optics and Short Pulse Spectroscopy, Max-Born-Str. 2a, 12489 Berlin, Germany
[*]chenweidong@fjirsm.ac.cn

Abstract: We report on sub-40 fs pulse generation from a Yb:Sc_2SiO_5 laser pumped by a spatially single-mode fiber-coupled laser diode at 976 nm. A maximum output power of 545 mW was obtained at 1062.6 nm in the continuous-wave regime, corresponding to a slope efficiency of 64% and a laser threshold of 143 mW. A continuous wavelength tuning across 80 nm (1030 -1110 nm) was also achieved. Implementing a SESAM for starting and stabilizing the mode-locked operation, the Yb:Sc_2SiO_5 laser delivered soliton pulses as short as 38 fs at 1069.5 nm with an average output power of 76 mW at a pulse repetition rate of ~79.8 MHz. The maximum output power was scaled to 216 mW for slightly longer pulses of 42 fs, which corresponded to a peak power of 56.6 kW and an optical efficiency of 22.7%. To the best of our knowledge, these results represent the shortest pulses ever achieved with any Yb^{3+}-doped rare-earth oxyorthosilicate crystal.

1. Introduction

Ytterbium (Yb^{3+}) doped rare-earth oxyorthosilicates with a general chemical formula Yb^{3+}:RE_2SiO_5 (where RE = Gd [1], Y [2], Lu [3], Sc [4] or their mixtures [5,6]), crystallize in the monoclinic system (sp. gr. $C2/c$ - C_{2h}^6). In the host lattice, Yb^{3+} ions can reside in two non-equivalent rare-earth sites of C_1 symmetry with VI- and VII-fold oxygen coordination and a strong distortion of the metal-ligand distances. This arrangement leads to strong crystal fields causing a relatively large Stark splitting of the ground ($^2F_{7/2}$) manifold [7] of the Yb^{3+} ions favoring relatively long emission wavelengths, increased Stark bandwidths and low laser threshold with weak temperature sensitivity. Monoclinic rare-earth oxyorthosilicate crystals are optically biaxial (positive) and provide polarized emission spectra. As host matrices, they feature high

#486560 https://doi.org/10.1364/OE.486560
Journal © 2023 Received 31 Jan 2023; revised 12 Mar 2023; accepted 17 Mar 2023; published 30 Mar 2023

thermal conductivities [8] favoring power scalable laser operation. Finally, the Yb^{3+}:RE_2SiO_5 crystals can be grown by the Czochralski method.

The broadband emission properties and good thermal behavior of Yb^{3+}:RE_2SiO_5 crystals make them extremely suitable for the development of high-power tunable and femtosecond lasers emitting in ~1 µm spectral range when pumping by commercial InGaAs laser diodes at ~980 nm [9–11]. For reaching sub-100 fs pulse durations with the Yb^{3+}:RE_2SiO_5 crystals, usually, Kerr-lens mode-locking (KLM) is implemented. Using Yb:Gd_2SiO_5 as a gain medium, 72 fs pulses were generated at 1050 nm via KLM corresponding to an average output power of 85 mW [12]. Slightly shorter pulse duration could be obtained with "mixed" (solid-solution) crystals as gain media. Diode-pumped KLM lasers generating pulses as short as 61 fs and 55 fs were demonstrated with Yb:$(Lu,Y)_2SiO_5$ [13] and Yb:$(Gd,Y)_2SiO_5$ [14]. Even shorter pulse duration of 54 fs was obtained from a diode-pumped KLM Yb:Lu_2SiO_5 laser with a central wavelength of 1052 nm and an average output power of 25 mW [15].

One of the well-known representatives of the rare-earth oxyorthosilicate laser crystals is the Yb^{3+}-doped scandium oxyorthosilicate Yb:Sc_2SiO_5 (shortly Yb:SSO). It exhibits a relatively higher thermal conductivity of 7.5 $Wm^{-1}K^{-1}$ (average value, for 1 at.% Yb^{3+} doping) at room temperature compared to its isotypes and a negative thermo-optic coefficient of -6.3×10^{-6} K^{-1} [8], which ensures good heat removal and a relatively weak thermal lensing effect when pumping with commercial high-power InGaAs laser diodes for power scalable laser operation. Yb^{3+} ions in this material exhibit large Stark splitting of the ground ($^2F_{7/2}$) manifold (1027 cm^{-1} [8]), which is attractive for low laser threshold laser operation. In addition, they show relative broad absorption zero-phonon line (ZPL) with a full width at half maximum (FWHM) of 24 nm at 976 nm, which releases the requirements for wavelength stabilization for high-power InGaAs laser diodes [8]. The broadband gain profiles and the moderate luminescence lifetime (0.7 ms) of Yb^{3+} ions in the Sc_2SiO_5 crystal make it very suitable for application in femtosecond regime, both in oscillators and amplifiers [4,16–18]. Power scalable operation in the femtosecond time domain would also be possible with the thin-disk configuration. A thin-disk Yb:Sc_2SiO_5 laser mode-locked (ML) with a SEmiconductor Saturable Absorber Mirror (SESAM) delivered a maximum average output power of 27.8 W with a pulse duration of 298 fs at 1036 nm [19].

In the present work, we explore the potential for sub-40 fs pulse generation from SESAM ML Yb:Sc_2SiO_5 lasers pumped by a spatially single-mode fiber-coupled InGaAs laser diode.

2. Laser set-up

An X-shaped astigmatically compensated linear cavity was used, see Fig. 1. A rectangular laser element was cut from the as-grown 4.4 at.% Yb^{3+}-doped Sc_2SiO_5 crystal (actual composition) grown by the Czochralski method [20–23] and oriented for light propagation along the optical indicatrix axis Y (Y-cut). It had an aperture of 3.3 mm × 3.3 mm and a thickness of 3 mm. This orientation was selected to benefit from high pump absorption efficiency under ZPL pumping. The laser element was mounted in a passively cooled copper holder using Indium foil for better heat removal and placed at Brewster's angle for $\boldsymbol{E} \parallel X$ polarization between two concave dichroic folding mirrors M_1 and M_2 (radius of curvature: RoC = -100 mm).

The pump source was a spatially single-mode, fiber-coupled InGaAs laser diode emitting unpolarized radiation at 976 nm. Its emission wavelength was locked using a Fiber Bragg grating (FBG) leading to a spectral linewidth (FWHM) of 0.2 nm. The pump beam was nearly diffraction-limited with a measured M^2 factor of ~1.02. The pump radiation was collimated using an aspherical lens L_1 (focal length: f = 25.4 mm) and then focused into the laser crystal through the M_1 mirror with a spherical focusing lens L_2 (f = 75 mm) resulting in a beam waist radius of 14 µm × 29 µm in the sagittal and tangential planes, respectively.

For continuous-wave (CW) laser operation, a four-mirror cavity was employed without a saturable absorber. One cavity arm was terminated by a flat end mirror M_3 and the other arm –

Optics EXPRESS

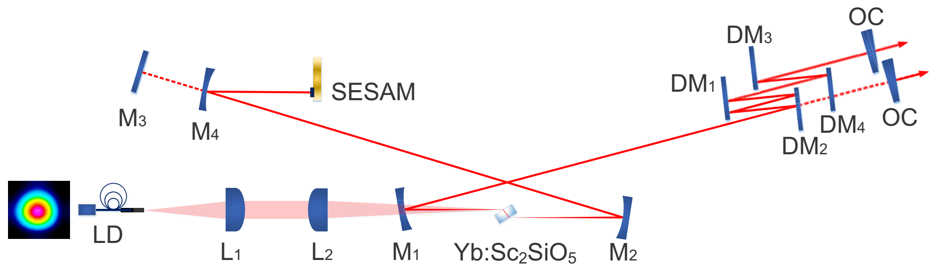

Fig. 1. Experimental layout of the Yb:Sc_2SiO_5 laser. LD: fiber-coupled laser diode at 976 nm; L_1: aspherical collimating lens; L_2: spherical focusing lens; M_1, M_2 and M_4: concave mirrors (RoC = -100 mm); M_3: flat end mirror; DM_1 – DM_4: flat dispersive mirrors; OC: output coupler. *Inset* – spatial profile of the pump radiation at full pump power.

by a plane-wedged output coupler (OC) with a transmission at the laser wavelength T_{OC} ranging from 1% to 7.5%. The cavity mode inside the laser cavity was simulated using the ray transfer matrix formalism yielding a waist radius in the laser crystal of 20 μm × 40 μm in the sagittal and tangential planes, respectively. The measured single-pass pump absorption under lasing conditions only slightly decreased with T_{OC} in the CW regime, from 72.8% to 71.7%.

For ML operation, the flat end mirror M_3 was substituted by a curved mirror M_4 (RoC = -100 mm) and the cavity arm was terminated by a commercial SESAM (BATOP, GmbH) with a modulation depth of ~0.6% at a central wavelength of 1040 nm (high reflection band: 1000 – 1070 nm), a non-saturable loss of ~0.4%, a saturation fluence of 70 μJ/cm^2, and a relaxation time of ~1 ps. The intracavity group delay dispersion (GDD) was managed by implementing four flat dispersive mirrors (DMs) characterized by a GDD per bounce of $DM_1 = DM_2$ = -150 fs^2 and $DM_3 = DM_4$ = -100 fs^2. The resulting total round-trip negative GDD amounted to -1600 fs^2 to compensate for the material dispersion and to balance the self-phase modulation (SPM) induced by the Kerr nonlinearity of the laser crystal. The physical length of the ML laser cavity was 1.88 m which corresponds to a pulse repetition rate of ~79.8 MHz.

3. Results and discussion

3.1. Continuous-wave laser operation

The Yb:Sc_2SiO_5 laser generated a maximum output power of 545 mW at 1062.6 nm with a slope efficiency η of 64% (*vs.* absorbed pump power using T_{OC} = 4.5%, see Fig. 2(a).

This corresponded to an absorbed pump power of 1.0 W and an optical efficiency of 54.5%. The laser threshold was 143 mW for this OC. The laser polarization was linear ($\boldsymbol{E}$ || X). Even higher η of 65.1% was obtained with a higher T_{OC} =7.5% reaching an output power of 500 mW at 1062 nm at an absorbed power of 0.99 W. The laser threshold increased with the output coupling, from 89 mW (T_{OC} = 1%) to 211 mW (T_{OC} = 7.5%). The laser wavelength in the CW regime experienced a slight blue-shift with increasing the OC transmission, from 1066 to 1062 nm, as shown in Fig. 2(c). This behavior is typical for quasi-three-level Yb lasers with inherent reabsorption at the laser wavelength and agrees with the gain spectra of Yb^{3+} ions in the Sc_2SiO_5 crystal.

The Caird analysis was applied to determine the passive losses in the Yb: Yb:Sc_2SiO_5 crystal: the measured laser slope efficiency was fitted as a function of -ln(R_{OC}), where $R_{OC} = 1 - T_{OC}$ is the output coupler reflectivity [24]. The analysis yielded the total round-trip cavity losses of δ = 0.28 ± 0.05% (reabsorption losses excluded) and an intrinsic slope efficiency η_0 of 74.4 ± 2%, as shown in Fig. 3(a).

Optics EXPRESS

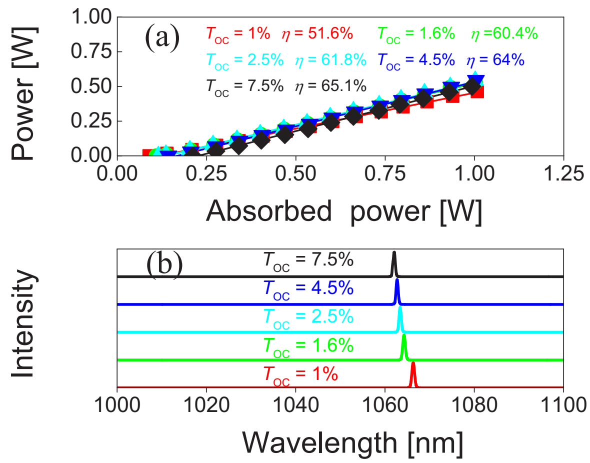

Fig. 2. CW Yb:Sc_2SiO_5 laser: (a) Input - output dependences for different OCs, η – slope efficiency; (b) Typical spectra of laser emission (laser polarization: $\boldsymbol{E} \parallel X$).

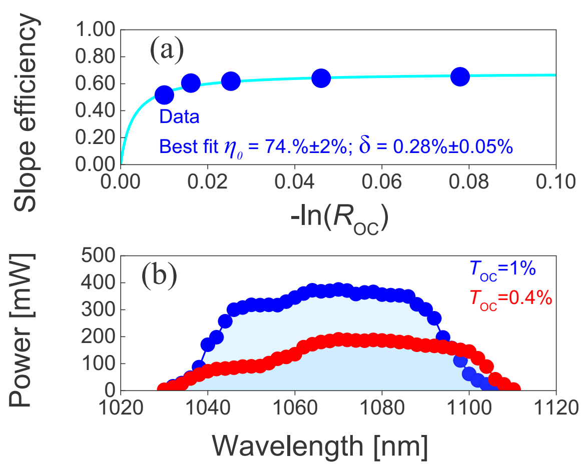

Fig. 3. CW Yb:Sc_2SiO_5 laser: (a) Caird analysis: laser slope efficiency plotted *vs.* -ln(R_{OC}); where $R_{OC} = 1 - T_{OC}$; (b) Laser tuning curves obtained with a Lyot filter, $T_{OC} = 0.4\%$ and 1%.

The potential of the Yb:Sc_2SiO_5 crystal for broadband wavelength tuning was studied in the CW regime by inserting a Lyot filter (a 2-mm thick quartz plate) at Brewster's angle close to the OC. The laser wavelength was continuously tunable between 1032 - 1106 nm, i.e., across 74 nm at the zero-power-level, for $T_{OC} = 1\%$ at an incident pump power of 1.5 W. For smaller $T_{OC} = 0.4\%$ at an incident pump power of 1.38 W, the tuning range was broader, 80 nm (1030 - 1110 nm), see Fig. 3(b). In this case, the power maximum of the tuning curve was observed at ~1070 nm.

The broadband tuning properties of Yb:Sc_2SiO_5 are due to the strong crystal-fields for the dopant Yb^{3+} ions in low-symmetry (C_1) sites in this crystal leading to a large total Stark splitting of the ground-state multiplet ($^2F_{7/2}$), namely 770 cm^{-1} (site I) and 1026 cm^{-1} (site II) [4]. Another reason is the spectral broadening due to the electron-phonon interaction.

Optics EXPRESS

3.2. Mode-locked laser operation

By implementing a commercial SESAM and four flat DMs into the laser cavity resulting in a total round-trip negative GDD of -1600 fs^2, stable and self-starting ML operation was readily achieved. The shortest pulses were obtained with a 1.6% OC. Their characterization is shown in Fig. 4.

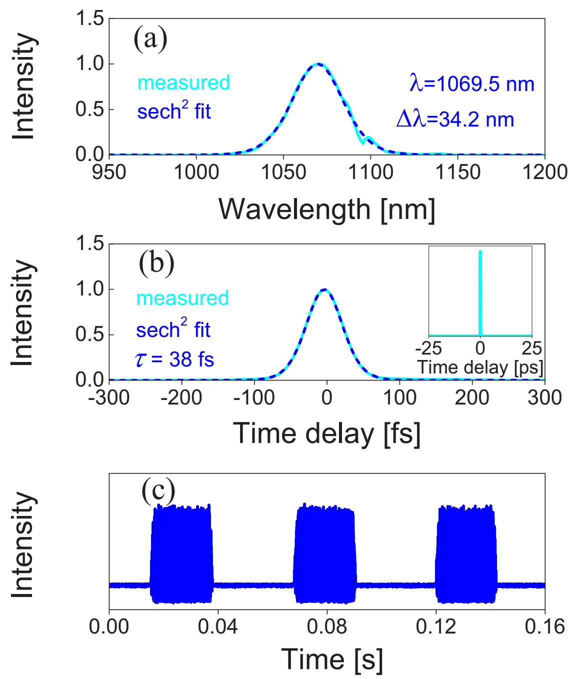

Fig. 4. SESAM ML $Yb:Sc_2SiO_5$ laser with $T_{OC} = 1.6\%$. (a) Optical spectrum; (b) SHG-based intensity autocorrelation trace, *dashed curve* - $sech^2$ fit. *Inset*: intensity autocorrelation trace measured on a time span of 50 ps; (c) Oscilloscope trace of the shortest pulse train measured with a 20-Hz chopper inserted into the intracavity beam, illustrating the self-starting operation.

The $Yb:Sc_2SiO_5$ laser delivered soliton pulses with an emission spectral bandwidth (FWHM) of 34.2 nm at a central wavelength of 1069.5 nm by assuming a $sech^2$-shape spectral intensity profile, see Fig. 4(a). The dip in the laser spectrum at ~1095 nm originates from the spectral profile of reflectivity of the used SESAM. The recorded second-harmonic generation (SHG) based intensity autocorrelation trace gave a deconvolved pulse duration of 38 fs (FWHM) assuming a $sech^2$-shaped temporal pulse profile, see Fig. 4(b). The corresponding time-bandwidth product (TBP) of 0.341 was slightly above the Fourier-transform-limit (0.315). A long-scale (50 ps) background-free intensity autocorrelation scan confirmed the single-pulse steady-state mode-locking, see the inset in Fig. 4(b). Under these conditions, an average output power of 76 mW was obtained at an absorbed pump power of 1.02 W (1.385 W incident pump power), corresponding to an optical efficiency of 7.5% and a peak power of 22.1 kW.

To emphasize the self-starting nature of mode-locking, a chopper rotating at a frequency of 20 Hz was inserted into the cavity and a fast photodetector was used to monitor the ML pulse train, see Fig. 4(c). The result well illustrates that the $Yb:Sc_2SiO_5$ laser was self-starting into a steady ML operation without any external perturbation.

A radio-frequency (RF) spectrum analyzer was used for confirming the stability of the ML operation for the shortest pulses. A relatively high extinction ratio of >71 dBc above the noise

Optics EXPRESS

level for the fundamental beat note at 79.81 MHz in combination with the uniform harmonics recorded on a 1-GHz frequency span provided evidence of highly stable CW-ML operation without any Q-switching or multi-pulsing instabilities, see Fig. 5.

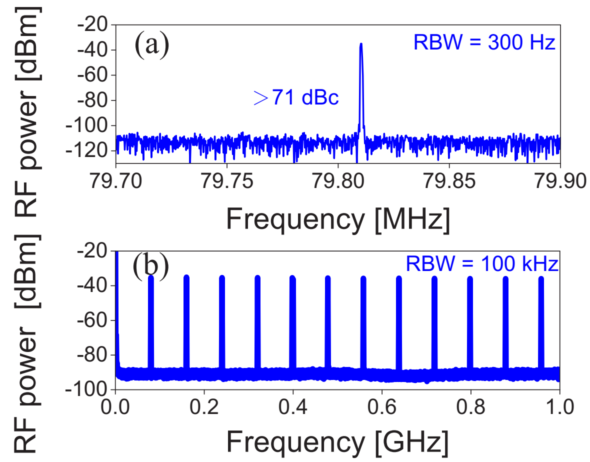

Fig. 5. RF spectra of the ML Yb:Sc_2SiO_5 laser with T_{OC} = 1.6%: (a) Fundamental beat note at 79.81 MHz recorded with a resolution bandwidth (RBW) of 300 Hz, and (b) harmonics on a 1-GHz frequency span recorded with a RBW of 100 kHz.

An IR camera was placed at 0.8 m away from the OC to record the far-field beam profiles both in the CW and ML regimes to reveal the dominating ML mechanism for generating the shortest pulse duration. The transition from CW to ML regime was accompanied by a slight shrinking of the beam size (diameter) from 1.50 (x) × 1.69 (y) mm^2 to 1.51 (x) × 1.56 (y) mm^2, as shown in Fig. 6. Such observation validated the underlying ML mechanism dominated by Kerr-lens mode-locking stabilized by the SESAM, which is supported by the high-brightness of the pump laser. However, the pulse shaping by the SESAM cannot be ruled out in view of the much wider stability zone and the self-starting mode-locking operation. Such a hybrid pulse shaping mechanism introduced an enhanced self-amplitude modulation (SAM) by the Kerr-lens effect, which assisted the SESAM ML operation for shorter pulse duration, i.e., Kerr-lens assisted SESAM ML operation.

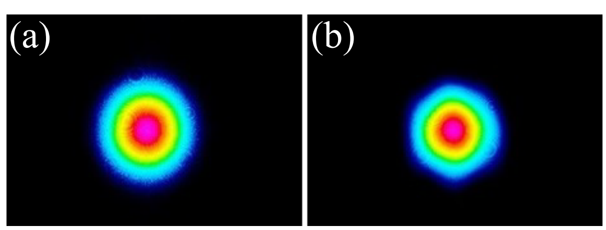

Fig. 6. Measured far-field beam profiles of the Yb:Sc_2SiO_5 laser (T_{OC} = 1.6%): (a) CW and (b) ML regimes of operation.

The scaling of the average output power from the ML laser was achieved by employing higher output coupling (T_{OC} = 4%) while the pulse duration was optimized by the total round-trip negative GDD of -1600 fs^2. The maximum average output power amounted to 216 mW (peak power 59.02 kW) for an absorbed pump power of 0.95 W (1.385 W incident pump power). The optical spectrum of ML laser was centered at 1068.1 nm with a sech^2-fitted spectral FWHM of 29.5 nm.

Optics EXPRESS

Pulses as short as 42 fs were obtained as confirmed by the measured SHG-based autocorrelation trace. The corresponding TBP was 0.326 still being close to the Fourier-transform-limit. The pulse repetition rate was ~79.83 MHz and the optical efficiency reached 22.7%.

4. Conclusion

To conclude, we report on sub-40 fs pulse generation from a passively mode-locked ytterbium scandium oxyorthosilicate (Yb:Sc_2SiO_5) laser pumped by a spatially single-mode fiber-coupled laser diode at 976 nm. Implementing a SESAM for starting and stabilizing the mode-locked operation, the Yb:Sc_2SiO_5 laser delivered soliton pulses as short as 38 fs at 1069.5 nm with an average output power of 76 mW and a pulse repetition rate of ~79.8 MHz, representing the shortest pulses ever achieved with any Yb^{3+}-doped rare-earth oxyorthosilicate crystals RE_2SiO_5 (parent or "mixed"). The mode-locking was self-starting. We suggest a hybrid pulse shaping mechanism with an enhanced self-amplitude modulation introduced by the Kerr-lens effect, which assisted the SESAM mode-locked operation resulting in a shorter pulse duration. Our results indicate the potential of the Yb:Sc_2SiO_5 crystal for Kerr-lens mode-locked lasers.

Funding. National Natural Science Foundation of China (61975208, 62205171, 61905247, U21A20508); Sino-German Scientist Cooperation and Exchanges Mobility Program (M-0040); National Key Research and Development Program of China (2021YFB3601504); MCIN/AEI/10.13 039/501100011033 (Agencia Estatal de Investigación) (PID2019-108543RB-I00).

Acknowledgment. Xavier Mateos acknowledges the Serra Húnter program.

Disclosures. The authors declare no conflicts of interest.

Data availability. Data underlying the results presented in this paper are not publicly available at this time but may be obtained from the authors upon reasonable request.

References

1. C. Yan, G. Zhao, L. Zhang, J. Xu, X. Liang, D. Juan, W. Li, H. Pan, L. Ding, and H. Zeng, "A new Yb-doped oxyorthosilicate laser crystal: Yb:Gd_2SiO_5," Solid State Commun. **137**(8), 451–455 (2006).
2. M. Jacquemet, C. Jacquemet, N. Janel, F. Druon, F. Balembois, P. Georges, J. Petit, B. Viana, D. Vivien, and B. Ferrand, "Efficient laser action of Yb:LSO and Yb:YSO oxyorthosilicates crystals under high-power diode-pumping," Appl. Phys. B **80**(2), 171–176 (2005).
3. G. Toci, A. Pirri, A. Beitlerova, Y. Shoji, A. Yoshikawa, J. Hybler, M. Nikl, and M. Vannini, "Characterization of the lasing properties of a 5%Yb doped Lu_2SiO_5 crystal along its three principal dielectric axes," Opt. Express **23**(10), 13210–13221 (2015).
4. R. Gaume, B. Viana, J. Derouet, and D. Vivien, "Spectroscopic properties of Yb-doped scandium based compounds Yb:$CaSc_2O_4$, Yb:$SrSc_2O_4$ and Yb:Sc_2SiO_5," Opt. Mater. (Amsterdam, Neth.) **22**(2), 107–115 (2003).
5. J. Du, X. Liang, Y. Xu, R. Li, Z. Xu, C. Yan, G. Zhao, L. Su, and J. Xu, "Tunable and efficient diode-pumped Yb^{3+}:GYSO laser," Opt. Express **14**(8), 3333–3338 (2006).
6. W. Li, S. Xu, H. Pan, L. E. Ding, H. Zeng, W. Lu, C. Guo, G. Zhao, C. Yan, and L. Su, "Efficient tunable diode-pumped Yb:LYSO laser," Opt. Express **14**(15), 6681–6686 (2006).
7. R. Gaume, P. Haumesser, B. Viana, D. Vivien, B. Ferrand, and G. Aka, "Optical and laser properties of Yb:Y_2SiO_5 single crystals and discussion of the figure of merit relevant to compare ytterbium-doped laser materials," Opt. Mater. (Amsterdam, Neth.) **19**(1), 81–88 (2002).
8. L. Zheng, J. Xu, G. Zhao, L. Su, F. Wu, and X. Liang, "Bulk crystal growth and efficient diode-pumped laser performance of Yb^{3+}:Sc_2SiO_5," Appl. Phys. B **91**(3-4), 443–445 (2008).
9. W. L. Tian, J. F. Zhu, Y. N. Peng, Z. H. Wang, L. H. Zheng, L. B. Su, J. Xu, and Z. Y. Wei, "High power sub 100-fs Kerr-lens mode-locked Yb:YSO laser pumped by single-mode fiber laser," Opt. Express **26**(5), 5962–5969 (2018).
10. F. Thibault, D. Pelenc, F. Druon, Y. Zaouter, M. Jacquemet, and P. Georges, "Efficient diode-pumped Yb^{3+}:Y_2SiO_5 and Yb^{3+}:Lu_2SiO_5 high-power femtosecond laser operation," Opt. Lett. **31**(10), 1555–1557 (2006).
11. W. Tian, Z. Wang, J. Zhu, L. Zheng, J. Xu, and Z. Wei, "Highly efficient and high-power diode-pumped femtosecond Yb:LYSO laser," Laser Phys. Lett. **14**(4), 045802 (2017).
12. W. Tian, Z. Wang, J. Zhu, L. Zheng, X. Xu, J. Xu, and Z. Wei, "Diode-pumped Kerr-lens mode-locked Yb:GSO laser generating 72 fs pulses," Opt. Laser Technol. **79**, 137–140 (2016).
13. W. L. Tian, Z. H. Wang, L. Wei, Y. N. Peng, J. W. Zhang, Z. Zhu, J. F. Zhu, H. N. Han, Y. L. Jia, L. H. Zheng, J. Xu, and Z. Y. Wei, "Diode-pumped Kerr-lens mode-locked Yb:LYSO laser with 61 fs pulse duration," Opt. Express **22**(16), 19040–19046 (2014).
14. J. Zhu, Z. Gao, W. Tian, J. Wang, Z. Wang, Z. Wei, L. Zheng, L. Su, and J. Xu, "Kerr-lens mode-locked femtosecond Yb:$GdYSiO_5$ laser directly pumped by a laser diode," Appl. Sci. **5**(4), 817–824 (2015).

15. W. Tian, Z. Wang, J. Zhu, Z. Wei, L. Zheng, X. Xu, and J. Xu, "Generation of 54 fs laser pulses from a diode pumped Kerr-lens mode-locked Yb:LSO laser," Chin. Phys. Lett. **32**(2), 024206 (2015).
16. W. Tan, D. Tang, J. Zhang, D. Shen, X. Xu, and J. Xu, "Dissipative soliton operation of an Yb^{3+}:Sc_2SiO_5 laser in the vicinity of zero group velocity dispersion," Opt. Photonics Lett. **05**(01), 1250001 (2012).
17. F. Pirzio, E. Caracciolo, M. Kemnitzer, A. Guandalini, F. Kienle, J. A. der Au, and A. Agnesi, "Performance of Yb:Sc_2SiO_5 crystal in diode-pumped femtosecond oscillator and regenerative amplifier," Opt. Express **23**(10), 13115–13120 (2015).
18. C. Xu, D. Tang, J. Zhang, H. Zhu, X. Xu, L. Zheng, L. Su, and J. Xu, "Sub-100 fs pulse generation in a diode pumped Yb:Sc_2SiO_5 laser," Opt. Commun. **294**, 237–240 (2013).
19. K. S. Wentsch, L. Zheng, J. Xu, M. A. Ahmed, and T. Graf, "Passively mode-locked Yb^{3+}:Sc_2SiO_5 thin-disk laser," Opt. Lett. **37**(22), 4750–4752 (2012).
20. Z. Zou, L. Zheng, J. Wang, D. Jiang, S. Liu, Q. Sai, J. Wang, H. Hu, and L. Su, "Crystal growth and photoluminescence spectra properties of $(Yb_xNd_ySc_{1-x-y})_2SiO_5$ laser crystal," Laser Phys. Lett. **15**(8), 085703 (2018).
21. Y. Zhao, Q. Wang, L. Meng, Y. Yao, S. Liu, N. Cui, L. Su, L. Zheng, H. Zhang, and Y. Zhang, "Anisotropy of the thermal and laser output properties in Yb,Nd:Sc_2SiO_5 crystal," Chin. Opt. Lett. **19**(4), 041405 (2021).
22. X. Liu, J. Guo, L. Zheng, J. Liu, Q. Peng, Y. Ge, and J. Xu, "Two - dimensional graphdiyne for passively Q-switched Yb^{3+}:Sc_2SiO_5 laser," Microw. Opt. Technol. Lett. **63**(9), 2292–2296 (2021).
23. L. Dong, Y. Yao, Q. Wang, S. Liu, L. Zheng, Y. Xu, D. Li, H. Zhang, Z. Zou, and L. Su, "Tunable and mode-locking Yb, Nd:Sc_2SiO_5 femtosecond laser," IEEE Photonics Technol. Lett. **30**(24), 2167–2170 (2018).
24. J. A. Caird, S. A. Payne, P. R. Staver, A. Ramponi, and L. Chase, "Quantum electronic properties of the $Na_3Ga_2Li_3F_{12}$:Cr^{3+} laser," IEEE J. Quantum Electron. **24**(6), 1077–1099 (1988).